

Electrochemistry and Homogeneous Self-Exchange Kinetics of the Aqueous 12-Tungstoaluminate(5–/6–) Couple

Almut Czap, Nancy I. Neuman, and Thomas W. Swaddle*

Department of Chemistry, University of Calgary, Calgary, Alberta, Canada T2N 1N4

Received March 28, 2006

The effect of alkali metal (M) chloride or triflate supporting electrolytes (0.1–1.0 mol L⁻¹) on the midpoint potential E_m of the aqueous $\text{AlW}_{12}\text{O}_{40}^{5-/6-}$ couple in cyclic voltammetry, after correction (E_{corr}) for liquid junction potentials, can be represented in terms of ionic strength according to the extended Debye–Hückel equation. However, unrealistically short $\text{AlW}_{12}\text{O}_{40}^{5-/6-}$ -cation closest-approach distances are required to accommodate the specific effects of M^+ , and the infinite-dilution potential E_{corr}^0 values are not quite consistent from one M^+ to another. The pressure dependence of E_m is qualitatively consistent with expectations based on the Born–Drude–Nernst theory. The strong accelerating effects of supporting electrolytes on the standard electrode reaction rate constant k_{el} at pH 3 as measured by alternating current voltammetry (ACV), and on the homogeneous self-exchange rate constant k_{ex} at pH 3–7 as measured by ²⁷Al line broadening, depend specifically on the identity and concentration of M^+ ($\text{Li}^+ < \text{Na}^+ < \text{K}^+ < \text{Rb}^+$) rather than on the ionic strength, whereas the effect of the nature of the supporting anion (Cl^- or CF_3SO_3^-) is negligible. Extrapolation of k_{el} and k_{ex} to zero $[\text{M}^+]$ indicates that the uncatalyzed electron transfer rate is negligibly small relative to the M^+ catalyzed rates. The kinetic effects of M^+ show no evidence of the saturation expected had they been due primarily to ion pairing with $\text{AlW}_{12}\text{O}_{40}^{5-/6-}$. The catalytic effect of M^+ operates primarily through lowering the enthalpy of activation, which is partially offset by a strongly negative entropy of activation and, for the homogeneous exchange catalyzed by K^+ or Rb^+ , becomes mildly negative; thus, the catalytic effect of M^+ is enthalpy-driven but entropy-limited. For the electrode reaction, the volume of activation averages $+4.5 \pm 0.2 \text{ cm}^3 \text{ mol}^{-1}$ for all M^+ and $[\text{M}^+]$, in contrast to the negative value predicted theoretically for the uncatalyzed reaction. These results are consistent with a reaction mechanism, previously proposed for other anion–anion electron-transfer reactions, in which anion–anion electron transfer is facilitated by partially dehydrated M^+ .

Introduction

Relationships between homogeneous self-exchange and heterogeneous (electrode) electron-transfer reaction kinetics in solution have recently been reviewed,¹ with particular attention to anion–anion electron-transfer reactions in aqueous solution as represented by cyanometalate couples. For those couples, both the electrode and homogeneous self-exchange reactions (rate constants k_{el} and k_{ex} , respectively) are catalyzed by alkali metal cations M^+ ($\text{M} = \text{Li} < \text{Na} < \text{K} < \text{Rb} < \text{Cs}$) to the effective exclusion of the uncatalyzed pathway. Quaternary ammonium ions R_4N^+ also catalyze homogeneous electron transfer between anions ($\text{Bu}_4\text{N}^+ < \text{Et}_4\text{N}^+ < \text{Me}_4\text{N}^+ \sim \text{Rb}^+ \text{ or } \text{Cs}^+$), but any comparable effect on the kinetics of heterogeneous electron-transfer reactions

is obscured by their tendency to adsorb on the electrode surface, blocking access of the electroactive species and possibly complicating observation of the electron-transfer process through slow desorption. The effect of the cations cannot be ascribed simply to ion pairing as such, since the cation concentration dependences of k_{ex} and k_{el} are often linear and do not show the thermodynamically predicted saturation. The pressure dependences of k_{ex} and k_{el} give positive values of the respective volumes of activation $\Delta V_{\text{ex}}^\ddagger$ and $\Delta V_{\text{el}}^\ddagger$ ($\Delta V_i^\ddagger = -RT(\partial \ln k_i/\partial P)_T$), whereas negative values are expected from Marcus theory for simple electron-transfer reactions. These facts are consistent with facilitation of electron transfer by partially dehydrated bridging cations: dehydration would be accompanied by a positive volume change, its energy requirements would give rise to the observed sequence of catalytic power of the alkali metal ions, the size effect seen with R_4N^+ (which do not require

* To whom correspondence should be addressed. E-mail: swaddle@ucalgary.ca. Phone: (403) 220-5358. Fax: (403) 289-9488.
(1) Swaddle, T. W. *Chem. Rev.* **2005**, *105*, 2573.

dehydration) is as expected for electron transfer via bulky bridges, and sequestration of M^+ with a crown ether or a cryptand destroys its catalytic power without changing the ionic strength.

These observations and their interpretation, however, derive almost entirely from studies of hexa- and octacyano-metalates, which are "soft" bases with extensive π electron systems, and the question arises as to whether "hard" anions such as oxoanions would behave similarly. Self-exchange in the MnO_4^{-2-} couple at constant ionic strength does show M^+ catalysis, but the effect is weaker than for cyanometalates in the sense that the uncatalyzed pathway is observable in competition with the M^+ -modulated path, and ΔV_{ex}^\ddagger for the former is more negative than can be easily explained;^{1,2} furthermore, attempts in our laboratory to measure the kinetics of the corresponding electrode reaction have been unsuccessful. More promising in this respect are the polyoxometalates, which are of major importance in their own right as redox catalysts (inter alia),³⁻⁷ and accordingly, any role played by the cations or a supporting electrolyte in the kinetics of their electron-transfer reactions needs to be delineated. For the aqueous 12-tungstocobaltate couple $CoW_{12}O_{40}^{5-6-}$, the electrode reaction does indeed exhibit specific cation catalysis ($Na^+ < K^+ < Rb^+ < Cs^+$) with positive ΔV_{el}^\ddagger ,⁸ but the kinetics of the corresponding homogeneous reaction are not easily measured (NMR is inapplicable because of the paramagnetism of both the 5- and 6- ions), and the validity of rate data obtained by a ^{60}Co radiotracer precipitation method⁹ has been questioned.⁶ The 12-tungstophosphate couples $PW_{12}O_{40}^{3-4-5-}$, although amenable to the use of ^{31}P NMR for determination of k_{ex} , are stable in water only at $pH < 1.5$ and in our experience are sufficiently soluble only in acidic solutions containing either Li^+ ($\leq 0.8 \text{ mol L}^{-1}$) or Na^+ ($< 0.5 \text{ mol L}^{-1}$) cations, offering only limited scope for the study of cation effects. Furthermore, the $PW_{12}O_{40}^{3-4-}$ self-exchange rate falls in the extreme fast limit on the ^{31}P NMR time scale, approaching diffusion control.^{8,10}

We have therefore turned our attention to the less familiar 12-tungstoaluminate couple $AlW_{12}O_{40}^{5-6-}$,¹¹⁻¹⁴ which is stable in aqueous solution up to $pH 7$ or higher, shows little

tendency to protonate in acidic solution, and is amenable to the use of ^{27}Al NMR for study of the self-exchange reaction kinetics; O_2 must, however, be rigorously excluded to avoid oxidation of $AlW_{12}O_{40}^{6-}$. A major question requiring discussion is whether the effect of electrolytes on k_{ex} can be accounted for entirely in terms of the extended Debye-Hückel theory, as proposed by Kozik and Baker¹⁰ for the self-exchange of $PW_{12}O_{40}^{3-4-}$ in $HCl/NaCl$ and adopted subsequently by Geletii et al.¹⁴ for that of $AlW_{12}O_{40}^{5-6-}$ in $NaCl$ media, or whether specific cation catalytic effects are dominant as they are in various cyanometalate systems.¹ An attempt is also made to assess the extent to which electrolyte effects on $AlW_{12}O_{40}^{5-6-}$ potentials and reaction kinetics might be accounted for in terms of ion pairing.

Experimental Section

Materials. $AlCl_3 \cdot 6H_2O$, $HClO_4$ (Baker Analyzed Reagent), $Na_2WO_4 \cdot 2H_2O$, $LiCl$, KCl , Celite, H_2SO_4 , $NaH_2PO_4 \cdot H_2O$, K_2HPO_4 (Fisher Scientific), $NaCl$, $NaOH$, KOH (EMD Chemicals), $LiOH \cdot H_2O$, LiH_2PO_4 , Na_2HPO_4 (Sigma-Aldrich), $RbCl$ (Sigma-Aldrich, 99.8% or 99.99%), Rb_2CO_3 (Sigma-Aldrich, 99.8%), and KH_2PO_4 (Baker and Adamson) were of ACS analytical reagent grade and were used without further purification. KCF_3SO_3 was made from CF_3SO_3H (Aldrich) by the method of Bonner.¹⁵ Crypt-2.2.2 (Aldrich), tetramethylammonium chloride (Eastman), tetraethylammonium bromide (Baker), and tetra-*n*-butylammonium bromide (Aldrich) were used as received. Distilled water was further purified on a Barnstead E-pure train. $\alpha-Na_5AlW_{12}O_{40}$ was prepared by the method of Weinstock et al.^{11,12,14} with a slight modification in the second step of the synthesis: the solution was kept at reflux usually for just 1 day instead of 6, leading to a higher yield and purity of the α -isomer (99.9%). $\alpha-K_5AlW_{12}O_{40}$ was obtained by replacing $NaOH$ by KOH in the final step of the synthesis. $\alpha-Li_5AlW_{12}O_{40}$ was obtained from $\alpha-Na_5AlW_{12}O_{40}$ by use of a Dowex 50W-X4 cation-exchange resin (BioRad). The progress of the syntheses was monitored by ^{27}Al NMR.

Electrochemical Measurements. pH measurements were made with an Orion model 420A pH meter, calibrated using standard buffer solutions. Liquid junction potentials were estimated from cell potentials, measured with a Hewlett-Packard 3468A multimeter relative to the $Ag/AgCl/NaCl(\text{satd})$ electrode, of a silver wire with a fresh electrolytic coat of $AgCl$ and immersed in MCl solution of the appropriate concentration thermostated at $25.0^\circ C$. Other electrochemical data were obtained using a CH Instruments model CHI650B electrochemical work station controlled by a computer (CHI software Version 4.08). The electrochemical cell was a conventional three electrode system: a $Ag/AgCl/NaCl(\text{satd})$ reference electrode and a gold wire (0.5 mm dia, Premion, Alfa Aesar) as counter and working electrode (flame sealed inside polyethylene tubes). Gold wire was used in preference to Pt, which appeared to catalyze decomposition of $AlW_{12}O_{40}^{5-}$, often giving a blue coloration of the solution near the electrode after a potential cycle. Before each experiment, the working electrode was gently polished with $0.05 \mu m$ Al_2O_3 polishing suspension (Buehler), followed by a potential cycling procedure in $1 \text{ mol L}^{-1} H_2SO_4$, as described elsewhere.^{16,17}

Cyclic voltammograms (CVs) and alternating current voltammograms (ACVs)¹ were obtained at selected temperatures (20–40

- (2) Spiccia, L.; Swaddle, T. W. *Inorg. Chem.* **1987**, *26*, 2265.
- (3) Pope, M. T. *Heteropoly and Isopoly Oxometalates*; Springer-Verlag: New York, 1983.
- (4) Pope, M. T.; Müller, A. *Polyoxometalates: From Platonic Solids to Anti-Retroviral Activity*; Kluwer Academic Publishers: Dordrecht, 1994.
- (5) *Polyoxometalate Chemistry: From Topology via Self-Assembly to Applications*; Pope, M. T.; Müller, A.; Eds.; Kluwer Academic Publishers: Dordrecht, 2001.
- (6) Weinstock, I. A. *Chem. Rev.* **1998**, *98*, 113.
- (7) Saha, S. K.; Ali, M.; Banerjee, P. *Coord. Chem. Rev.* **1993**, *122*, 41.
- (8) Matsumoto, M.; Neuman, N. I.; Swaddle, T. W. *Inorg. Chem.* **2004**, *43*, 1153.
- (9) Rasmussen, P. G.; Brubaker, C. H., Jr. *Inorg. Chem.* **1964**, *3*, 977.
- (10) Kozik, M.; Baker, L. C. W. *J. Am. Chem. Soc.* **1990**, *112*, 7604.
- (11) Cowan, J. J.; Hill, C. L.; Reiner, R. S.; Weinstock, I. A. *Inorg. Synth.* **2002**, *33*, 18.
- (12) Weinstock, I. A.; Cowan, J. J.; Barbuzzi, E. M. G.; Zeng, H.; Hill, C. L. *J. Am. Chem. Soc.* **1999**, *121*, 4608.
- (13) Cowan, J. A.; Bailey, A. J.; Heintz, R. A.; Do, B. T.; Hardcastle, K. I.; Hill, C. L.; Weinstock, I. A. *Inorg. Chem.* **2001**, *40*, 6666.
- (14) Geletii, Yu. V.; Hill, C. L.; Bailey, A. J.; Hardcastle, K. I.; Atalla, R. H.; Weinstock, I. A. *Inorg. Chem.* **2005**, *44*, 8955.

- (15) Bonner, O. D. *J. Am. Chem. Soc.* **1981**, *103*, 3262.
- (16) Sawyer, D. T.; Sobkowiak, A.; Roberts, J. R., Jr. *Electrochemistry for Chemists*, 2nd ed.; Wiley: New York, 1995.
- (17) Fu, Y.; Swaddle, T. W. *J. Am. Chem. Soc.* **1997**, *119*, 7137.

°C) using a glass-jacketed cell thermostated with circulating water (± 0.1 °C). All measurements were made under Ar with strict exclusion of O₂. All sample solutions were prepared with 0.005 mol L⁻¹ tungstoaluminate and 0.001 mol L⁻¹ HClO₄ or HCl. LiCl, NaCl, KCl, KCF₃SO₃, or RbCl was added in concentrations of 0.1, 0.2, 0.3, 0.5, 0.7, or 1.0 mol L⁻¹ as supporting electrolytes (however, AlW₁₂O₄₀⁵⁻ formed a precipitate with [RbCl] > 0.3 mol L⁻¹ or [KCF₃SO₃] > 0.7 mol L⁻¹). The cation of the tungstoaluminate salt used was the same as that of the added electrolyte except in the case of Rb: crystalline α -Rb₅AlW₁₂O₄₀ was insufficiently soluble, and α -K₅AlW₁₂O₄₀ was therefore used with RbCl as supporting electrolyte. The uncompensated resistance R_u of the cell for a particular solution was measured either directly at 10 kHz at a potential 200–300 mV away from that of the redox couple to be studied or with the CHI software (with close agreement), and was used to correct the CVs and ACVs subsequently measured, either manually or automatically using the CHI software.¹⁸ CVs were recorded at 4–5 different sweep rates ν in the range 10–100 mV s⁻¹ for M = Na and K, or at 50 and 100 mV s⁻¹ for M = Li and Rb, to determine the CV midpoint potentials $E_m = (E_{pa} + E_{pc})/2$, where E_{pa} and E_{pc} are the potentials of the current extrema of the anodic and cathodic sweeps relative to Ag/AgCl/saturated NaCl. E_m values were found to be independent of ν and reproducible to ± 1 mV.

ACVs were run at different frequencies f (5–120 Hz), recording the in-phase and 90°-out-of-phase (quadrature) voltammograms. Rate constants k_{el} , calculated from the phase angle φ of the AC peak current as described below, are the averages of at least three runs at different frequencies. The surface area of the working electrode was determined by using a standard solution of 0.004 mol L⁻¹ Fe(CN)₆³⁻ in aqueous 1.0 mol L⁻¹ KCl which has a known diffusion coefficient of $(7.63 \pm 0.01) \times 10^{-6}$ cm² s⁻¹ at 25 °C.¹⁶

Experiments at elevated pressure (0–200 MPa) were performed in similar fashion at 25.0 ± 0.1 °C using a thermostated high-pressure electrochemical cell assembly, essentially that previously described¹⁷ but with minor redesign of the cell (Figure S1, Supporting Information). E_m values measured in the high-pressure assembly at 0.1 MPa against the internal Ag/AgCl/NaCl(satd) reference electrode agreed with those measured using the conventional glass cell. Care was taken that the results obtained at the start and at the end of a pressure cycle were in good agreement, specifically, that E_m values agreed to within ± 2 mV.

NMR Measurements. ²⁷Al NMR spectra were obtained using a Bruker AMX300-WB spectrometer operating at 78.20 MHz. The temperature readout was calibrated against the ¹H chemical shifts of methanol and ethylene glycol.¹⁹ Nuclear longitudinal relaxation times T_1 were measured using a standard 180°/90° pulse sequence and Bruker XWINNMR software.

Solutions containing the requisite M₅AlW₁₂O₄₀ (5 mmol L⁻¹) and MCl or MCF₃SO₃ salts in 20% D₂O were reduced under Ar in a BASi electrolysis cell comprising a reticulated glassy carbon working electrode, a coiled Pt wire counter electrode, and a Ag/AgCl reference electrode, to give AlW₁₂O₄₀^{5-/6-} solutions containing a mole fraction x of the reduced species at the potential $E = E_m + (RT/nF)\ln[(1-x)/x]$. A MH₂PO₄/M₂HPO₄ buffer (0.050 mol L⁻¹) was incorporated in the solutions to counteract the pH change that otherwise would accompany electrolysis.²⁰ In unbuffered solutions, the pH rose by about 2 pH units during electrolysis, to a maximum pH of 8.5, whereas in the buffered solutions the pH

remained between 6.5 and 7.0. In fact, the UV-vis spectrum of the AlW₁₂O₄₀⁵⁻ anion (molar absorbance maximum 2.50×10^4 L mol⁻¹ cm⁻¹ at 262 nm) was constant over several hours at pH 9.5, implying that any pH variability associated with electrolysis was quite acceptable. For M = Rb, Li₅AlW₁₂O₄₀ was used with RbCl, as solid Rb₅AlW₁₂O₄₀ was too poorly soluble, and because of limited solubilities 1.0 mmol L⁻¹ HCl was used in place of phosphate buffer.

Solution samples were degassed under vacuum with three freeze–pump–thaw cycles in a NMR tube fitted with a J. Young valve. Rigorous exclusion of O₂ from the AlW₁₂O₄₀^{5-/6-} system was necessary to prevent slow reoxidation of the reduced anion. The reaction of AlW₁₂O₄₀⁶⁻ with O₂ was faster in the presence of K⁺ and especially Rb⁺ supporting electrolytes than in Na⁺ media similar to those used by Geletii et al.,¹⁴ leading ultimately to formation of a fine white precipitate over the course of an NMR experiment. Following electrolytic reduction of AlW₁₂O₄₀⁵⁻ under Ar, a solution sample was withdrawn with a Hamilton gastight syringe and quickly introduced to a 5 mm Ar-filled NMR sample tube (Wilmad grade 528-PP) on a Schlenk line through a three-way T-bore stopcock; the sample was then degassed with three freeze–pump–thaw cycles, and the tube was flame-sealed under vacuum. Samples so prepared appeared to be stable indefinitely at room temperature.

²⁷Al NMR chemical shifts were referred to an external sample of [Al(H₂O)₆]Cl₃ solution (0.1 mol L⁻¹; chemical shift $\delta = 0$). Shimming was done on the ¹H channel, and the internal 20% D₂O provided a ²D lock signal. A 90° pulse width of 18 μ s was applied in all ²⁷Al spectra. For AlW₁₂O₄₀⁵⁻ in 20% D₂O at 28 °C, T_1 was found to be 2.3 ± 0.2 s, and accordingly, delay times of 12 s ($\sim 5T_1$) were applied between pulses to ensure accurate line width measurements. Broad background ²⁷Al resonances at $44 \leq \delta \leq 97$ ppm with much shorter T_1 times, due to Al in probehead components and the sample tube, were removed by digital background subtraction of a blank spectrum or, as a check, by left-shifting the FID (with the same result).

Results and Discussion

The potentials and rate constants presented below showed no dependence on pH over the range used in these experiments, in agreement with the observation of Geletii et al.¹⁴ who concluded that neither AlW₁₂O₄₀⁵⁻ nor AlW₁₂O₄₀⁶⁻ is significantly protonated even in acidic solutions. Results were independent of the sources of the reagents.

Electrode Potentials for AlW₁₂O₄₀^{5-/6-}: Electrolyte Dependence. The solubility of the aluminotungstates with [RbCl] > 0.3 mol L⁻¹, [KCF₃SO₃] > 0.7 mol L⁻¹, and in all CsCl media was too low, and the rate of the electrode reaction in LiCl media below 0.3 mol L⁻¹ was too slow (i.e., the CV peaks were too broad and E_{pa} and E_{pc} were too far apart), for accurate collection of midpoint potentials E_m . Since, for consistency, all E_m measurements were made relative to the Ag/AgCl/NaCl(satd) electrode, estimates of the liquid junction potentials E_{ij}^{MCl} via measurement of the potentials E^{MCl} of Ag/AgCl/MCl/NaCl(satd)/AgCl/Ag cells could be made accurately only for NaCl media, for which there is both a common anion and cation at the junction. In this case, E_{ij}^{NaCl} is given by $(2t_+ - 1)E^{NaCl}/2t_+$,²¹ where t_+ is

(18) He, P.; Faulkner, L. R. *Anal. Chem.* **1986**, *58*, 517.

(19) (a) Günther, H. *NMR Spectroscopy*; Wiley: Chichester, U. K., 1980.

(b) Van Geet, A. L. *Anal. Chem.* **1968**, *40*, 2227.

(20) Macka, M.; Andersson, P.; Haddad, P. R. *Anal. Chem.* **1998**, *70*, 743.

(21) Glasstone, S. *An Introduction to Electrochemistry*; Van Nostrand: New York, 1942; pp 203–210.

Table 1. Parameters Representing the Effects of the Electrolyte MX and Pressure on the Midpoint Potential and Electrode Reaction Rate Constant of the Aqueous AlW₁₂O₄₀^{5-/6-} Couple at a Gold Wire Electrode^a

MX	[MX]/mol L ⁻¹	<i>E</i> _m /mV	<i>E</i> _{corr} ^b /mV	Δ <i>H</i> _{Ag/AgCl} ^c /kJ mol ⁻¹	Δ <i>S</i> _{Ag/AgCl} ^c /J K ⁻¹ mol ⁻¹	Δ <i>V</i> _{Ag/AgCl} /cm ³ mol ⁻¹	<i>k</i> _{el} /10 ⁻² cm s ⁻¹	Δ <i>V</i> _{el} [‡] /cm ³ mol ⁻¹
LiCl	0.3	-377 ^d	-357				0.66 ± 0.01	
	0.5	-367 ^e	-350	15 ± 1	-67 ± 3	-30.3 ± 0.9	0.79 ± 0.02 ^f	4.6 ± 0.1
	0.7	-357 ^e	-342				1.07 ± 0.01	
	1.0	-350 ^e	-336	16 ± 1	-58 ± 1	-28.0 ± 0.8	1.44 ± 0.02 ^f	4.4 ± 0.1
NaCl	0.10	-384	-359	16 ± 1	-69 ± 3		0.90 ± 0.02 ^f	
	0.20	-371	-350	12 ± 1	-79 ± 2	-28.1 ± 0.6	2.29 ± 0.06 ^f	4.6 ± 0.1
	0.30	-363	-344				2.58 ± 0.01	
	0.50	-350	-333	15 ± 1	-63 ± 3	-28.1 ± 0.5	4.85 ± 0.06 ^f	4.5 ± 0.1
	0.70	-343	-328				7.23 ± 0.01	
	1.00	-331	-317	14 ± 1	-59 ± 1	-28.4 ± 0.9	10.2 ± 0.3 ^f	4.8 ± 0.4
KCl	0.10	-375	-351	20 ± 1	-55 ± 1	-24.6 ± 0.7	2.41 ± 0.07 ^f	4.5 ± 0.2
	0.20	-359	-340	16 ± 1	-63 ± 2	-27.6 ± 0.8	4.32 ± 0.05	4.9 ± 0.2
	0.30	-351	-334				6.78 ± 0.01	
	0.50	-336	-323	13 ± 1	-64 ± 3	-25.3 ± 0.7	11.8 ± 1.0 ^f	4.7 ± 0.2
	0.70	-328	-317				15.4 ± 0.1	
	1.00	-315	-306	12 ± 1	-63 ± 2	-25.7 ± 1.0	31.6 ± 0.6 ^f	4.0 ± 0.1
KCF ₃ SO ₃	0.10	-376 ^e					2.29 ± 0.03	
	0.20	-362 ^e					4.37 ± 0.25	
	0.30	-356 ^e					6.61 ± 0.07	
	0.50	-336 ^e				-23.5 ± 1.2	11.6 ± 0.07	5 ± 1
	0.70	-328 ^e					15.7 ± 0.3	
RbCl	0.1	-369 ^e	-345	15 ± 1	-68 ± 2	-27.4 ± 0.5	2.43 ± 0.05 ^{f,g}	4.5 ± 0.1
	0.2	-354 ^e	-335	16 ± 1	-62 ± 1	-26.7 ± 0.6	6.24 ± 0.09 ^{f,g}	4.4 ± 0.1
	0.3	-343 ^e	-326				12.7 ± 0.1 ^g	

^a 25.0 °C; 0.1 MPa (except Δ*V*_{el}[‡]: mean value 0–200 MPa); [M₅AlW₁₂O₄₀] = 5.0 mmol L⁻¹; [HCl] or [HClO₄] = 1.0 mmol L⁻¹; ionic strength *I* = [MX] + 0.076 mol L⁻¹; scan rate for CVs = 10–100 mV s⁻¹ (average of 4–7 measurements) except as indicated; all potentials are relative to Ag/AgCl/saturated NaCl, uncorrected for the liquid junction potential except as noted; to convert *E*_m or *E*_{corr} to formal potentials vs NHE, add 192 mV. ^b Adjusted for liquid junction potential (Table S1). ^c From *E*_m = (*T*Δ*S*_{Ag/AgCl} - Δ*H*_{Ag/AgCl})/*F*. ^d CV scan rate = 50 mV s⁻¹. ^e CV scan rate 100 mV s⁻¹. ^f Recalculated for 25.0 °C from Δ*H*_{el}[‡] and Δ*S*_{el}[‡] (Table S6). ^g Corrected for the contribution of the K⁺ counterion (0.44 × 10⁻² cm s⁻¹).

the transport number of aqueous Na⁺ (0.392 at 25 °C and moderately low [NaCl]¹⁶). Values of *E*_{ij}^{NaCl}, calculated with the approximation that *t*₊ can be taken as concentration-independent, are collected in Table S1 in the Supporting Information. For the other chloride media, in which M⁺ differs from the reference electrode cation, it was found that *E*^{MCl} values were not very different from *E*^{NaCl} at the same concentration (Table S1), evidently because the junction properties were dominated by NaCl(satd) (~6.3 mol L⁻¹). Accordingly, it may be assumed that the small differences in *E*^{MCl} between MCl and NaCl systems were due solely to liquid junction effects, so that *E*_{ij}^{MCl} is given approximately by *E*_{ij}^{NaCl} - (*E*^{MCl} - *E*^{NaCl}) (Table S1). The corrected CV midpoint potential *E*_{corr} is then *E*_m - *E*_{ij}^{MCl}. For KCF₃SO₃ media, neither the anion nor the cation was common with that of the reference electrode, and no liquid junction corrections were attempted. For Δ*V*_{el}[‡], any contribution from liquid junction potentials can be ignored,²² as a consequence of the near-independence of the viscosity of aqueous solutions on pressure (0–200 MPa) at near-ambient temperatures.¹

The dependence of *E*_m, *E*_{corr}, *k*_{el}, and related parameters on the identity and concentration of the supporting electrolyte MX is summarized in Table 1, which shows clearly that these quantities are sensitive to the nature of M⁺ but not X⁻ (Cl⁻ vs CF₃SO₃⁻). The Ag/AgCl/NaCl(satd) reference electrode measured -7 mV relative to Ag/AgCl/KCl(satd) (+199 mV vs NHE¹⁶), and accordingly *E*_m and *E*_{corr} values of Table 1 can be converted to conventional formal electrode potentials

relative to NHE by addition of 192 mV. Values of Δ*H*_{Ag/AgCl} and Δ*S*_{Ag/AgCl} from *FE*_m = *T* Δ*S*_{Ag/AgCl} - Δ*H*_{Ag/AgCl} are included in Table 1 simply to represent the temperature dependences of *E*_m relative to Ag/AgCl/NaCl(satd), and have not been corrected for liquid junction effects.

In principle, the dependence of *E*_{corr} on the ionic strength *I* (= [MCl] + 15[M₅AlW₁₂O₄₀] + [HClO₄]) can be related to the ionic charge numbers *z* and anion-cation closest approach distances *a* through single-ion activity coefficients *γ*_{*z*} calculated from an adaptation of the extended Debye-Hückel equation:^{23,24}

$$\ln \gamma_z = -[Az^2 I^{1/2}/(1 + BaI^{1/2})] \quad (1)$$

$$\begin{aligned} E_{\text{corr}} &= E_{\text{corr}}^0 + (RT/F) \ln (\gamma_{5-}/\gamma_{6-}) \\ &= E_{\text{corr}}^0 + [332.1I^{1/2}/(1 + 3.286aI^{1/2})], \end{aligned} \quad (2)$$

in mV at 25 °C for *a* in nm

For water at a given temperature and pressure, *A* and *B* are exactly calculable from theory (1.1751 L^{1/2} mol^{-1/2} and 3.2856 L^{1/2} mol^{-1/2} nm⁻¹, respectively, at 25.0 °C and 0.1 MPa), and the liquid-junction-corrected “infinite dilution” midpoint potential *E*_{corr}⁰ should be the same for all the

(23) (a) Debye, P.; Hückel, E. *Phys. Z.* **1923**, *24*, 185. (b) Debye, P.; Hückel, E. *Phys. Z.* **1923**, *24*, 305. (c) Hückel, E. *Phys. Z.* **1925**, *26*, 93.

(24) (a) Robinson, R. A.; Stokes, R. H. *Electrolyte Solutions*, 2nd ed. revised; Butterworth: London, 1965; p 230. (b) Harned, H. S.; Owen, B. B. *The Physical Chemistry of Electrolytic Solutions*, 3rd ed.; Reinhold: New York, 1958; pp 64–66. (c) Bockris, J. O'M.; Reddy, A. K. N. *Modern Electrochemistry, Ionics*; Kluwer: New York, 1998; Vol. 1, pp 273–292.

(22) Swaddle, T. W.; Tregloan, P. A. *Coord. Chem. Rev.* **1999**, *187*, 255.

Table 2. Parameters Relating to Equations 2 and 4, Representing the Ionic Strength Dependence of the Liquid-Junction-Corrected $\text{AlW}_{12}\text{O}_{40}^{5-/6-}$ Potential in Chloride Media

M	Li	Na	K	Rb
$E_{\text{corr}}^0/\text{mV},^a$ from fit to eq 2	-452 ± 8	-440 ± 3	-433 ± 2	-428 ± 3
a/nm , from fit to eq 2	0.58 ± 0.07	0.54 ± 0.02	0.51 ± 0.02	0.50 ± 0.04
$r_{\text{cryst}}/\text{nm}^b$	0.076	0.105	0.138	0.149
$r_{\text{hyd}}/\text{nm}^c$	0.23	0.179	0.122	
$r_{\text{hyd}}/\text{nm}^d$	0.382	0.358	0.331	0.329
$r_{\text{hyd}}/\text{nm}^e$	0.41	0.34	0.33	0.32
$r_{\text{hyd}}/\text{nm}^f$	0.358	0.276	0.188	0.178
a_{th}/nm , theoretical ^f	0.918	0.836	0.748	0.738
$E_{\text{corr}}^0/\text{mV},^a$ from fit to eq 4 ^g	-435 ± 3	-427 ± 1	-422 ± 1	-420 ± 1
$c/\text{mV L mol}^{-1}$, from fit to eq 4 ^g	15 ± 4	18 ± 1	17 ± 1	30 ± 4

^a Relative to Ag/AgCl/saturated NaCl. ^b For six-coordination; ref 26. ^c Reference 29. ^d Reference 30. ^e Reference 31. ^f Reference 32, slip limit. ^g Using a_{th} values calculated from slip-limit M^+ radii of ref 32.

supporting electrolytes. The ion size (distance of closest approach) parameter a is often regarded simply as an adjustable parameter that acknowledges qualitatively that ions are not point charges,^{24c} but in accordance with Brønsted's principle of specific interaction of ions²⁵ a should reflect the sum of the effective radii in solution of the 12-tungstoaluminate anion and the relevant cation.^{23c,24c} The relevant ionic dimensions are the hydrated radii (r_{hyd}) rather than the crystallographic radii²⁶ (r_{cryst}). For $\alpha\text{-AlW}_{12}\text{O}_{40}^{5-}$, r_{hyd} may be equated to its hydrodynamic radius of 0.56 ± 0.04 nm (obtainable from its diffusion coefficient, see below), which turns out to be the same as both r_{hyd} of the isostructural $\alpha\text{-SiW}_{12}\text{O}_{40}^{4-}$ ion^{27,28} and r_{cryst} for $\alpha\text{-AlW}_{12}\text{O}_{40}^{5-}$ ion,¹² consistent with the notion that the interactions of polyoxometalate ions with solvent water are weak.^{10,14} For the alkali metal cations M^+ , some reported values of r_{hyd} are given in Table 2.^{29–32} There is evident disagreement regarding the numerical values of r_{hyd} for M^+ , attributable³² to the use of the Stokes–Einstein relation

$$r_{\text{hyd}} = k_{\text{B}}T/X\pi D\eta \quad (3)$$

to estimate r_{hyd} from measurements of the ionic diffusion coefficient D and solvent viscosity η , since the parameter X may have a value anywhere from 6, as in the original Stokes model in which solvent “sticks” to the surface of the diffusing ion, to 4 in the “slip” limit. The choice of $X = 4$ avoids the unrealistic result that $r_{\text{hyd}} < r_{\text{cryst}}$ for the larger alkali-metal cations (that is, r_{hyd} then allows for solvent that is already “stuck” to the ion), and accordingly, the “slip” values of r_{hyd} ³² are adopted to calculate a_{th} , the theoretical values of a , in Table 2. The actual closest approach distance, however, may

- (25) Brønsted, J. N. *Trans. Faraday Soc.* **1927**, 23, 416.
 (26) Shannon, R. D. *Acta Crystallogr.* **1976**, A32, 751.
 (27) Kurucsev, T.; Sargeson, A. M.; West, B. O. *J. Phys. Chem.* **1957**, 61, 1567.
 (28) Pope, M. T.; Varga, G. M., Jr. *Inorg. Chem.* **1966**, 5, 1249.
 (29) Cox, W. M.; Wolfenden, J. H. *Proc. R. Soc. London, Ser. A* **1934**, 145, 475.
 (30) Nightingale, E. R., Jr. *J. Phys. Chem.* **1959**, 63, 1381.
 (31) Prue, J. E.; Sherrington, P. J. *Trans. Faraday Soc.* **1961**, 57, 1795.
 (32) Paul, P. C. F.; Berg, J. O.; McMillan, W. G. *J. Phys. Chem.* **1990**, 94, 2671.

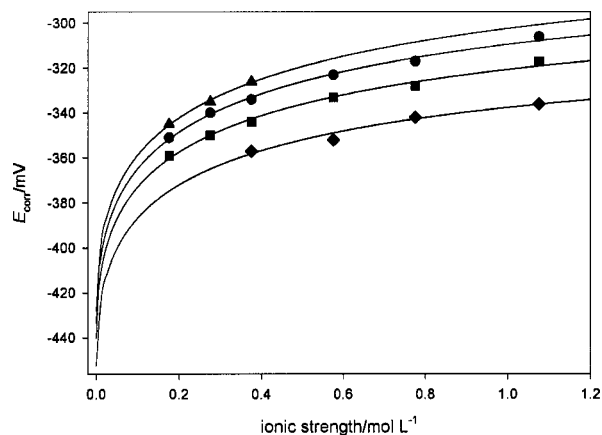


Figure 1. Fit of liquid-junction-corrected midpoint potentials to eq 2 at 25.0 °C, treating the ion size parameter a as empirically adjustable. Supporting electrolyte: LiCl (◆), NaCl (■), KCl (●), RbCl (▲).

be less than a_{th} if partial dehydration of M^+ occurs on contact with an anion, and in any event values of a obtained from experiment have been found to be somewhat concentration-dependent, so undermining the purpose of eq 2.^{24c}

Nonlinear least-squares fits of E_{corr} and I from Table 1 to eq 2 gave the curves shown in Figure 1 and the E_{corr}^0 and a values listed in Table 2. The requirements of our experiments (moderately high concentrations of supporting electrolyte to mitigate double layer and ion migration effects and of $M_{5/6}\text{AlW}_{12}\text{O}_{40}$ for comparison with the NMR experiments) prevented measurements at low ionic strengths where E_{corr} is predicted to depend sharply on I ; thus, the extrapolated E_{corr}^0 values are not expected to be precise. Nevertheless, it is clear that eq 2 represents the curvature of the E_{corr} versus I plots well, but fails to account adequately for the specific effects of the various M^+ , resulting in a considerable spread values of E_{corr}^0 (-452 to -428 mV) and values of a that are all much less than the expected values a_{th} (and in some cases less than the radius of $\text{AlW}_{12}\text{O}_{40}^{5-}$ alone).

These shortcomings of eq 2 are not surprising, as the supporting electrolyte concentrations required to minimize double-layer, resistance, and ion migration effects in our experiments gave ionic strengths in excess of the 0.1 mol L^{-1} limit up to which the Debye–Hückel treatment is normally considered valid. A common stratagem to extend the concentration range of eq 2 is to add an empirical term cI on the right-hand side:^{24a,24b,25}

$$E_{\text{corr}} = E_{\text{corr}}^0 + 332.1I^{1/2}/(1 + 3.286aI^{1/2}) + cI \quad (4)$$

If a is fixed at the theoretical values a_{th} for each M^+ (Table 2) and the E_{corr} data of Table 1 are fitted to eq 4, a correlation at least as satisfactory as that in Figure 1 is obtained (Figure S2 in the Supporting Information), giving more consistent E_{corr}^0 values (bottom of Table 2) averaging -426 ± 3 mV. An objectionable feature of eq 4, however, is that the limitations of eq 2 are transferred from a to the purely empirical additional parameter c , with consequent loss of predictive power.

It may be conjectured that c reflects anion–cation pairing, which would deplete the concentration of the “free” $6-$ ion

more than that of the 5⁻, leading to E_{corr} values more positive than are predicted by the extended Debye–Hückel equation without the c term, an effect that would be partially offset by the expected decline in the ion pair formation constants K_{IP} with rising ionic strength. Indeed, for the $\text{SiVW}_{11}\text{O}_{40}^{5-}$ ion and its reduced form in aqueous *tert*-butyl alcohol, experimental ion pair formation constants for pairing with M^+ increase significantly in the order $\text{M} = \text{Li} < \text{Na} < \text{K}$.³³ There is, however, no clear evidence for ion pairing by polyoxotungstates in undiluted water,^{10,14} which has a higher dielectric constant than aqueous *tert*-butyl alcohol. For guidance, rough theoretical ion-pair formation constants K_{IP} for aqueous 12-tungstoaluminates can be calculated from the Fuoss equation³⁴ (Table S2, Supporting Information) using the theoretical a_{th} data of Table 2. The Fuoss K_{IP} values at practical ionic strengths suggest that ion pairing for the $\text{AlW}_{12}\text{O}_{40}^{5-/6-}/\text{M}^+$ system is neither extensive enough to be considered saturated, nor so limited that the fraction of pairs could be either neglected or taken to be proportional to $[\text{M}^+]$. Table S2 shows that K_{IP} declines quite sharply as the ionic strength increases from zero, but the ratio $K_{\text{IP}}^{6-}/K_{\text{IP}}^{5-}$ is only about 2.2–2.6 even at infinite dilution and falls to 1.2–1.3 at $I \sim 1.0$. In a hypothetical limiting scenario in which ion pairing is near saturation at all I , the depletion of $[\text{M}^+]$ is neglected, and only the unpaired tungstoaluminate ions contribute to E_{corr} , ion pairing increases E_{corr} by a maximum amount $\Delta E_{\text{IP}} = (RT/F)\ln(K_{\text{IP}}^{6-}/K_{\text{IP}}^{5-})$, calculated values of which are given in Table S2. On this basis, the greatest effect ion pairing could have on E_{corr} at the ionic strengths of our study is 4–7 mV, with little variation with I or the identity of M^+ , even though the Fuoss K_{IP} values themselves are not negligible. This would explain why Geletii et al.¹⁴ found no potentiometric evidence for ion pairing between $\text{AlW}_{12}\text{O}_{40}^{5-/6-}$ and Na^+ , even though some degree of pairing is expected.

It may be noted that ion pairing between chloride (the major anion in most of our experiments) and alkali metal ions is known to be negligible in aqueous solutions at near-ambient temperatures and concentrations up to about 1 mol L⁻¹.³⁵

In summary, the curvature of the ionic strength dependence of E_{corr} for the $\text{AlW}_{12}\text{O}_{40}^{5-/6-}$ couple with various M^+ can be satisfactorily represented by extended Debye–Hückel theory, but only if either physically unrealistic values of the ion size parameter a are adopted (eq 2), which may be a further indication that the parameter a has no precise physical meaning,^{22,36,37} or an empirical term cI is added (eq 4). In either case, the variation in E_{corr} with the nature of M^+ is not fully accounted for (i.e., the apparent values of the

infinite-dilution potential E_{corr}^0 are not quite the same for all M^+), and ion pairing as predicted by the Fuoss equation can accommodate only a minor part of the differences. Excessive ionic strengths apart, Debye–Hückel-based theories may fail in the case of polyoxometalate ions because the charges and ionic radii are both much larger than were envisaged in the theoretical development, and furthermore it may not be appropriate to include the disproportionately large contributions of these ions in the computed ionic strength.

Alternatives to the extended Debye–Hückel treatment of electrolyte effects, such as that of Pitzer which is effective for concentrations up to 6 mol kg⁻¹,³⁸ introduce empirical parameters which impede their use in developing successors to eqs 2 and 4. Abbas et al.³⁹ have recently reviewed these alternative treatments, and have shown that their own corrected Debye–Hückel (CDH) theory, which focuses upon van der Waals properties for short-range ion–ion interactions and the traditional Debye–Hückel approach for longer-range electrostatic effects and in which the mean ionic diameter is the only empirical parameter, is effective for simple 1:1, 2:1, and 3:1 (but not 2:2) electrolytes in concentrations of up to about 1 mol L⁻¹. Application of the CDH theory in the present context, however, is unlikely to provide useful alternatives to eq 2 or the related kinetics equations considered below because of its added complexity; moreover, the issue of meaningful ionic sizes emerges once again.

Electrode Potentials for $\text{AlW}_{12}\text{O}_{40}^{5-/6-}$: Temperature and Pressure Dependences. The temperature dependences of E_{m} are summarized in Table 1 as enthalpies $\Delta H_{\text{Ag}/\text{AgCl}}$ and entropies $\Delta S_{\text{Ag}/\text{AgCl}}$ of reaction relative to the $\text{Ag}/\text{AgCl}/\text{NaCl}(\text{satd})$ electrode, from $E_{\text{m}} = (T\Delta S_{\text{Ag}/\text{AgCl}} - \Delta H_{\text{Ag}/\text{AgCl}})/F$. No large variations or unequivocal trends are evident, although $\Delta H_{\text{Ag}/\text{AgCl}}$ appears to diminish with increasing I , at least for K^+ . These parameters are uncorrected for the liquid junction potentials, and detailed interpretation is not warranted.

The pressure dependences of E_{m} at 25.0 °C were linear (typical examples are given in the Supporting Information, Figures S3 and S4) and are represented in Table 1 as volumes of reaction $\Delta V_{\text{Ag}/\text{AgCl}} = -F(\partial E_{\text{m}}/\partial P)_T$,²² which contain a contribution from the Ag/AgCl electrode and again show no clear pattern of dependence on the nature or the concentration of the supporting electrolyte. The pressure dependence of the liquid junction potentials can be neglected.²² The average $\Delta V_{\text{Ag}/\text{AgCl}}$ for $\text{AlW}_{12}\text{O}_{40}^{5-/6-}$ is $-27.3 \pm 1.6 \text{ cm}^3 \text{ mol}^{-1}$, which may be compared with -14 to $-16 \text{ cm}^3 \text{ mol}^{-1}$ for $\text{PW}_{12}\text{O}_{40}^{3-/4-}$ and $-25.5 \text{ cm}^3 \text{ mol}^{-1}$ for $\text{PW}_{12}\text{O}_{40}^{4-/5-}$,⁸ in qualitative agreement with the expectation from Born–Drude–Nernst theory^{8,22,36,37} that $\Delta V_{\text{Ag}/\text{AgCl}}$ should be linearly related to the change $\Delta(z^2/r)$ on reduction, where z is the charge on the oxidized form and r is its effective radius, if solvational change is the dominant factor.

(33) Grigoriev, V. A.; Cheng, D.; Hill, C. L.; Weinstock, I. A. *J. Am. Chem. Soc.* **2001**, *123*, 5292.

(34) $\ln K_{\text{IP}} = (-1.671 \times 10^7 z_+ z_- a/\epsilon T) + \ln(2.523 \times 10^{-9} a^3)$, where ϵ is the dielectric constant of the medium and a is in pm. Fuoss, R. M. *J. Am. Chem. Soc.* **1958**, *80*, 5059.

(35) (a) Harned, H. S.; Owen, B. B. *The Physical Chemistry of Electrolytic Solutions*, 3rd ed.; Reinhold: New York, 1958; pp 383 and 422. (b) Pettit, G.; Pettit, L.; Powell, K. J. *IUPAC Stability Constants Database*; Academic Software: Otley, West Yorkshire, U. K.

(36) Matsumoto, M.; Swaddle, T. W. *Inorg. Chem.* **2004**, *43*, 2724 and references therein.

(37) Yu, B.; Lever, A. B. P.; Swaddle, T. W. *Inorg. Chem.* **2004**, *43*, 4496.

(38) (a) Pitzer, K. S. *J. Phys. Chem.* **1973**, *77*, 268. (b) Pitzer, K. S. In *Activity Coefficients in Electrolyte Solutions*; Pytkowicz, R. M., Ed.; CRC Press: Boca Raton, FL, 1979; Vol. 1, pp 157–208.

(39) Abbas, Z.; Gunnarsson, M.; Ahlberg, E.; Nordholm, S. *J. Phys. Chem. B* **2002**, *106*, 1403.

This means $\Delta V_{\text{Ag}/\text{AgCl}}$ should become more negative with increasingly negative z , since r usually does not change much. For $\text{CoW}_{12}\text{O}_{40}^{5-/-6-}$, $\Delta V_{\text{Ag}/\text{AgCl}}$ is about $-22 \text{ cm}^3 \text{ mol}^{-1}$, with some small dependence on the added electrolyte,⁸ but in that case the electron is added specifically to the central high-spin Co^{III} atom on reduction, possibly leading to a Jahn–Teller-type expansion, whereas in the $\text{AlW}_{12}\text{O}_{40}^{6-}$ ion the added electron is delocalized over the 12 outer WO_6 units⁶ with zero unpaired electron density at the Al nucleus, as shown by the equal, narrow ($<1 \text{ Hz}$) ^{27}Al NMR line widths of $\text{AlW}_{12}\text{O}_{40}^{5-}$ and $\text{AlW}_{12}\text{O}_{40}^{6-}$ as discussed below. For cyanometalates, $\Delta V_{\text{Ag}/\text{AgCl}}$ values of about -36 , -33 , -30 , and $-28 \text{ cm}^3 \text{ mol}^{-1}$ are reported for $\text{Fe}(\text{CN})_6^{3-/-4-}$, $\text{Os}(\text{CN})_6^{3-/-4-}$, $\text{Mo}(\text{CN})_8^{3-/-4-}$, and $\text{W}(\text{CN})_8^{3-/-4-}$, respectively;²² these ions, however, are all much smaller than the 12-tungstometalates, so that $\Delta(z^2/r)$ is more negative for the cyanometalates than for $\text{AlW}_{12}\text{O}_{40}^{5-/-6-}$ despite their less negative z . As elsewhere,^{1,8,20,36,37} however, we caution against attempting to apply the Born–Drude–Nernst relation quantitatively, as there is much uncertainty surrounding meaningful values for r (cf. the discussion of a , above).

Diffusion Coefficients. Mean diffusion coefficients D for $\text{AlW}_{12}\text{O}_{40}^{5-/-6-}$, required for the calculation of k_{el} , were obtained from current extrema in CVs but showed some scatter attributable to inconsistent evaluation of the gold electrode surface area by the $\text{Fe}(\text{CN})_6^{3-/-4-}$ calibrant. A mean value of $D = 4.5 \times 10^{-6} \text{ cm}^2 \text{ s}^{-1}$ (standard error 8%) was obtained at $25.0 \text{ }^\circ\text{C}$ with sweep rates of both 50 and 100 V s^{-1} for 10 solutions containing MCl ($M = \text{Li, Na, K, Rb}$) at various representative concentrations. This value is effectively identical with that calculated from eq 3 with $X = 6$ using the accepted radius of 0.56 nm for $\text{AlW}_{12}\text{O}_{40}^{5-/-14}$ ($D = 4.4 \times 10^{-6} \text{ cm}^2 \text{ s}^{-1}$, adopted here), and it is consistent with values reported for other isostructural polyoxometalate anions at various electrolyte concentrations.^{8,28,40,41} In principle, the supporting electrolyte and its concentration can influence D through its effect on η (eq 3), but for MCl solutions⁴² of the concentrations used in this study η is not sufficiently different from that of pure water for this effect to be of consequence in calculating k_{el} , which depends on $D^{1/2}$. Indeed, for $\text{CoW}_{12}\text{O}_{40}^{5-/-6-}$, the effect of MCl on D was barely discernible.⁸

At $25 \text{ }^\circ\text{C}$, the pressure dependence of D was negligible, as has been found for other electroactive aqueous solutes,^{1,43} reflecting the fact that η for water is fortuitously almost independent of pressure at this temperature. The dependence of D on temperature, calculated from eq 3 using the viscosity of water reported by Sengers and Kamgar-Parsi,⁴⁴ is given in Table S3 (Supporting Information).

Kinetics of the $\text{AlW}_{12}\text{O}_{40}^{5-/-6-}$ Electrode Reaction: Electrolyte Effects. Standard electrode reaction rate constants k_{el} were obtained from ACV measurements of the maximum in-phase and quadrature currents at small ($1\text{--}5 \text{ mV}$) imposed AC potentials of frequency f , giving the corrected phase angle φ as described elsewhere.¹ Measurements were limited to the reaction at gold electrodes, as some decomposition appeared to occur at Pt electrodes and rate data obtained at glassy carbon electrodes were less reproducible. For the slowest reactions (in the less concentrated LiCl media), the CV peak separations $E_{\text{pa}} - E_{\text{pc}}$ became wide enough for estimation of k_{el} by the Nicholson method, but as found with other systems,¹ the results were much less precise than those from ACV though they were roughly consistent with them. The transfer coefficient α was obtained from the potential E_{max} of the current maximum in ACVs using eq 5

$$E_{\text{max}} = E_{\text{m}} + (RT/F)\ln[\alpha/(1 - \alpha)] \quad (5)$$

whence, if ω is the angular AC frequency ($=2\pi f$)

$$\cot \varphi = 1 + (2D\omega)^{1/2}/\alpha \bar{E} \alpha (1 - \bar{E} \alpha)^{\bar{E}(1-\bar{E}\alpha)} k_{\text{el}} \quad (6)$$

In practice, α was close to 0.50 at all temperatures, pressures, and electrolyte concentrations covered in this study (Table S4, Supporting Information), so that eq 6 reduces to

$$k_{\text{el}} = (D\omega/2)^{1/2}/(\cot \varphi - 1). \quad (7)$$

Because inadequate correction for the uncompensated resistance R_{u} can give rise to artifacts that masquerade as electrode reaction kinetics,^{1,45} values of R_{u} generated by the CHI software¹⁸ (Table S5, Supporting Information) were checked against direct measurements made at 10 kHz , and good agreement was found. R_{u} was about 80% larger in the high-pressure cell (the configuration of which was necessarily less than optimal) than in the glass cell used for the variable-temperature study. In general, however, R_{u} was quite small, especially at the higher electrolyte concentrations and temperatures, and any errors in measurements of E_{m} or k_{el} due to current- R_{u} potentials would have been negligible.⁸ Moreover, R_{u} , like D , showed very little variation with pressure (Table S5), so that any impact of R_{u} on $\Delta V_{\text{el}}^{\ddagger}$ would have been entirely negligible.

Values of k_{el} and the associated enthalpies $\Delta H_{\text{el}}^{\ddagger}$, entropies $\Delta S_{\text{el}}^{\ddagger}$, and volumes $\Delta V_{\text{el}}^{\ddagger}$ of activation are collected in Tables 1 and S6 (Supporting Information). In the $\text{AlW}_{12}\text{O}_{40}^{5-/-6-}$ system, values of k_{el} below about $0.007 \text{ cm}^2 \text{ s}^{-1}$ were too low for accurate measurement by the ACV method, and consequently, no reliable data were obtainable for LiCl media with $[\text{LiCl}] \leq 0.2 \text{ mol L}^{-1}$, or for $[\text{NaCl}] = 0.1 \text{ mol L}^{-1}$ at variable pressure (for which increasing pressure retarded the already slow reaction). Poor solubility precluded measurements with $M = \text{Cs}$ or with $[\text{RbCl}] > 0.3 \text{ mol L}^{-1}$. Nevertheless, Table 1 shows that k_{el} increases with $[\text{MCl}]$ and, at constant $[\text{MCl}]$, in the sequence $M = \text{Li} < \text{Na} < \text{K}$

(40) Baker, M. C.; Lyons, P. A.; Singer, S. J. *J. Am. Chem. Soc.* **1955**, *77*, 2011.

(41) Baker, L. C. W.; Pope, M. T. *J. Am. Chem. Soc.* **1960**, *82*, 4176.

(42) (a) Kaminsky, M. *Discuss. Faraday Soc.* **1957**, *24*, 171. (b) Kaminsky, M. *Z. Phys. Chem. N. F.* **1956**, *8*, 173. (c) Kaminsky, M. *Z. Phys. Chem. N. F.* **1957**, *12*, 206.

(43) Fu, Y.; Cole, A. S.; Swaddle, T. W. *J. Am. Chem. Soc.* **1999**, *121*, 10410.

(44) Sengers, J. V.; Kamgar-Parsi, B. *J. Phys. Chem. Ref. Data* **1984**, *13*, 185.

(45) Weaver, M. J. *Chem. Rev.* **1992**, *92*, 463.

< Rb, but is independent of the identity of the anion of the supporting electrolyte (Cl^- vs CF_3SO_3^-). The question now arises as to whether these phenomena are attributable to the ionic strength I or are specific cation effects.

In principle, the ionic strength dependence of the rate constant k of a bimolecular reaction between ions of charge numbers z_1 and z_2 in homogeneous solution is given by the Brønsted–Bjerrum–Christiansen (BBC) equation⁴⁶

$$\ln(k^I/k^{I=0}) = 2Az_1z_2I^{1/2}/(1 + BaI^{1/2}) \quad (8)$$

which is derived from eq 1 by assuming the anion–cation closest-approach distance a to be the same for both the reactants and the transition state. As a derivative of extended Debye–Hückel theory, eq 8 is not expected to be accurate at $I > 0.1 \text{ mol L}^{-1}$, but it was nevertheless used by Kozik and Baker¹⁰ and Geletii et al.¹⁴ to analyze the ionic strength dependence of the homogeneous self-exchange rates of $\text{PW}_{12}\text{O}_{40}^{3-/4-}$ and $\text{AlW}_{12}\text{O}_{40}^{5-/6-}$, respectively, in aqueous HCl/NaCl media; we comment further on this choice below. For an electrode reaction in which an ion of charge z and anion–cation closest approach distance a reacts with an electron on an electrode of effectively infinite radius to form a transition state of charge $(z - 1)$ at constant a , the procedure used to derive eq 8 gives

$$\ln(k_{\text{el}}^I/k_{\text{el}}^{I=0}) = (1 - 2z)AI^{1/2}/(1 + BaI^{1/2}) \quad (9)$$

For reduction of $\text{AlW}_{12}\text{O}_{40}^{5-}$ at an electrode at 25.0 °C, the right-hand side of eq 9 becomes $12.925I^{1/2}/(1 + 3.286aI^{1/2})$ if a is in nanometers. Although nonlinear least-squares fits of the k_{el} values of Table 1 to eq 9 reproduced the curvature of $\ln k_{\text{el}}$ vs I plots satisfactorily for each individual M^+ , the resulting infinite-dilution values of $k_{\text{el}}^{I=0}$ varied unacceptably with M^+ (Figure S5) and the values of the ion size parameter a so obtained were unrealistic, being smaller than the radius of $\text{AlW}_{12}\text{O}_{40}^{5-}$ itself ($a/\text{nm} = 0.47, 0.37, 0.38$ and 0.13 for $\text{M} = \text{Li}, \text{Na}, \text{K}$ and Rb , respectively) and hence much smaller than the theoretical ion size parameters a_{th} (Table 2). Nonlinear regressions of the observed $\ln k_{\text{el}}$ data on eq 9 using values of a_{th} from Table 2 with incorporation of an arbitrary additional term CI on the right-hand side (cf. eq 3), as advocated by Pethybridge and Prue,⁴⁶ failed to represent the curvature of the $\ln k_{\text{el}}$ vs I plots satisfactorily and gave unacceptably scattered values of $k_{\text{el}}^{I=0}$. Alternative treatments based on the Pitzer³⁸ and CDH³⁹ procedures would be excessively complex and would introduce further adjustable parameters.

Fits of k_{el} to either eq 9 or a quadratic in I or $[\text{M}^+]$ showed that its value at zero I or $[\text{M}^+]$ would be negligible in relation to the experimental uncertainty; that is, that the rate of the electrode reaction in the absence of M^+ (e.g., if M^+ were sequestered) would be too slow to measure by our procedures. Accordingly, for the purpose of summarizing the data empirically without resort to a prejudicial model and testing the closeness of approach of the dependence of k_{el} on $[\text{M}^+]$ to direct proportionality as has been found for some

cyanometalate systems,¹ one can resort to a power fit (eq 10, and Figure S6 in the Supporting Information) that emphasizes the role of M^+ rather than ionic strength and involves no assumptions about ionic sizes.

$$k_{\text{el}} = m[\text{M}^+]^p \quad (10)$$

Nonlinear least-squares fits of k_{el} to eq 10 gave $m/\text{cm L}^p \text{ mol}^{-p} \text{ s}^{-1} = 0.0142 \pm 0.0001, 0.0974 \pm 0.0023, 0.242 \pm 0.006$, and 0.915 ± 0.124 , with $p = 0.93 \pm 0.03, 1.08 \pm 0.05, 1.15 \pm 0.06$, and 1.65 ± 0.10 for LiCl, NaCl, KCl, and RbCl, respectively. Thus, k_{el} is effectively directly proportional to $[\text{M}^+]$ for $\text{M} = \text{Li}$ and Na at least.

At constant ionic strength, k_{el} increases in the sequence $\text{M} = \text{Li} < \text{Na} < \text{K} < \text{Rb}$ much more sharply than can be accounted for in terms of physically rational values of a in eq 9, and consequently, the effect of the supporting electrolyte on k_{el} cannot be ascribed to Debye–Hückel-type medium effects alone. By the same token, a plausible mechanism by which electron transfer would occur exclusively via stable ion pairs cannot account for the specific influence of M^+ , insofar as the theoretical anion–cation closest-approach distances a_{th} in Table 2 are appropriate and the Fuoss equation³⁴ is applicable. For most of our data, the ionic strength exceeds the accepted limit of applicability of the extended Debye–Hückel theory, but a marked dependence of k_{el} on the nature of M^+ is nevertheless evident even at $[\text{MCl}] = 0.1 \text{ mol L}^{-1}$.

Comparison of k_{el} values for $\text{AlW}_{12}\text{O}_{40}^{5-/6-}$ with the corresponding data for $\text{CoW}_{12}\text{O}_{40}^{5-/6-}$ in KCl media indicates a greater sensitivity of $\text{AlW}_{12}\text{O}_{40}^{5-/6-}$ relative to the Co system to external cation effects (data for the latter couple in RbCl solutions are qualitative at best). This may be attributed to the involvement of a peripheral molecular orbital of the tungstoaluminate in electron transfer rather than a deep-seated Co-centered one as in $\text{CoW}_{12}\text{O}_{40}^{5-/6-}$ (cf. discussion of $\Delta V_{\text{Ag}/\text{AgCl}}$ above and $\Delta V_{\text{el}}^\ddagger$ below).

Kinetics of the $\text{AlW}_{12}\text{O}_{40}^{5-/6-}$ Electrode Reaction: Temperature and Pressure Effects. Although solvent-dynamical control of electrode reaction rates is important in nonaqueous media, conventional transition-state theory seems to be valid for electrode kinetics in undiluted aqueous solutions.¹ Accordingly, the enthalpy $\Delta H_{\text{el}}^\ddagger$ and entropy $\Delta S_{\text{el}}^\ddagger$ of activation for the $\text{AlW}_{12}\text{O}_{40}^{5-/6-}$ electrode reaction (Table 1) were calculated from the Eyring equation

$$k_{\text{el}} = (k_{\text{B}}T\kappa/h) \exp[(\Delta S_{\text{el}}^\ddagger/R) - \Delta H_{\text{el}}^\ddagger/RT] \quad (11)$$

in which κ is the transmission coefficient (taken to be 1) and the other symbols have their usual meanings. In this standard form, which was developed for homogeneous systems, the pre-exponential factor is not strictly applicable to electrode kinetics, and the discrepancy will appear as a modest constant offset in the apparent $\Delta S_{\text{el}}^\ddagger$, although $\Delta H_{\text{el}}^\ddagger$ is a quantitatively valid parameter.

Figure 2 summarizes values of $\Delta H_{\text{el}}^\ddagger$ and $\Delta S_{\text{el}}^\ddagger$ (tabulated in Table S6, Supporting Information). Within the experimental uncertainty, $\Delta H_{\text{el}}^\ddagger$ decreases markedly in the sequence $\text{M} = \text{Li} \geq \text{Na} > \text{K} > \text{Rb}$ but shows no significant

(46) Pethybridge, A. D.; Prue, J. E. *Prog. Inorg. Chem.* **1972**, *17*, 327.

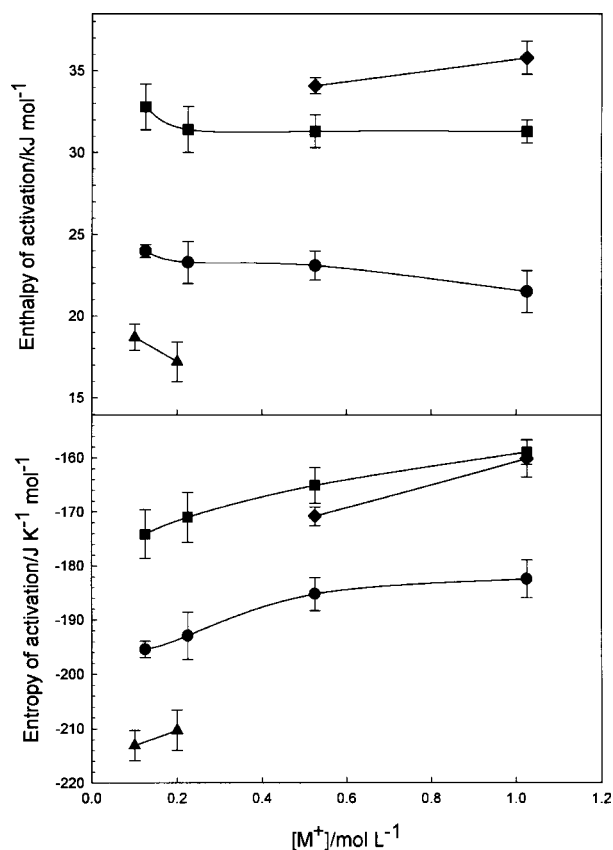


Figure 2. Influence of the nature and concentration of the cation on ΔH_{el}^\ddagger (top panel) and ΔS_{el}^\ddagger for the $\text{AlW}_{12}\text{O}_{40}^{5-/6-}$ electrode reaction in MCl media. M = Li (◆), Na (■), K (●), Rb (▲). For M = Rb, the contributions of the pathway involving the K^+ counterion of the tungstoaluminate ($[\text{K}^+] = 0.025 \text{ mol L}^{-1}$) have been subtracted.

dependence (within the uncertainty limits of the error bars) on the supporting electrolyte concentrations, whereas ΔS_{el}^\ddagger increases with $[\text{M}^+]$. As we go from M = Na to K and then Rb, the decrease in ΔH_{el}^\ddagger is partially offset by a parallel decrease in ΔS_{el}^\ddagger (Figure 2 and Table S6), a further example of the familiar phenomenon of enthalpy–entropy compensation. However, on balance it is seen that the influence of the nature of M^+ on k_{el} for the $\text{AlW}_{12}\text{O}_{40}^{5-/6-}$ couple is predominantly an enthalpic effect whereas the concentration effect of a particular M^+ acts mainly through ΔS_{el}^\ddagger . This is consistent with a mechanism, previously proposed,¹ in which electron transfer to and from anions occurs with the involvement of a partially dehydrated M^+ ion, since the enthalpies of hydration of M^+ become less negative in the sequence $\text{Li} < \text{Na} < \text{K} < \text{Rb}$.⁴⁷

Support for this mechanism comes from the effect of pressure on k_{el} for $\text{AlW}_{12}\text{O}_{40}^{5-/6-}$; examples of the linear $\ln k_{ex}$ versus P plots for a slow (LiCl medium) and a fast (RbCl medium) exchange are given in Figures S3 and S4. In all cases, the volume of activation ΔV_{el}^\ddagger is positive, averaging $+4.5 \pm 0.2 \text{ cm}^3 \text{ mol}^{-1}$ (Table 1). For simple electron transfer in aqueous media at an electrode, ΔV_{el}^\ddagger is expected to be negative, both from an extension of Marcus theory and from observational experience.¹ For the highly charged AlW_{12} -

$\text{O}_{40}^{5-/6-}$ couple, the theoretical calculation is numerically unstable because the negative Coulombic and positive Debye–Hückel contributions become large at the experimental ionic strengths, but a value of ΔV_{el}^\ddagger of about $-2 \text{ cm}^3 \text{ mol}^{-1}$ can be estimated (numerically small because of the large radii of the reacting anions) for the electrode reaction in absence of any specific involvement of M^+ .¹ If partial dehydration of M^+ is a prerequisite for its involvement in the electron-transfer process, it will make a substantial positive contribution to ΔV_{el}^\ddagger .^{1,48}

On the other hand, the rather small but nearly constant ΔV_{el}^\ddagger values for $\text{AlW}_{12}\text{O}_{40}^{5-/6-}$ stand in contrast to the larger values for $\text{CoW}_{12}\text{O}_{40}^{5-/6-}$ reported earlier.⁸ For $\text{CoW}_{12}\text{O}_{40}^{5-/6-}$, ΔV_{el}^\ddagger also shows a marked dependence on the nature of M^+ and a small decrease with rising $[\text{M}^+]$ that are not evident with $\text{AlW}_{12}\text{O}_{40}^{5-/6-}$. The dehydration mechanism would suggest relatively large ΔV_{el}^\ddagger values with a small but measurable dependence on the nature of M^+ , as is seen for the cobaltate couple. The key difference between the $\text{CoW}_{12}\text{O}_{40}^{5-}$ and $\text{AlW}_{12}\text{O}_{40}^{5-}$ reductions is that the added electron goes to the Co^{III} center in the former ion, probably causing additional volume changes as proposed above for $\Delta V_{Ag/AgCl}$, but is delocalized over the tungstate periphery of the latter.⁶ A less positive ΔV_{el}^\ddagger for $\text{AlW}_{12}\text{O}_{40}^{5-/6-}$ is therefore understandable, and any dependence on M^+ may be obscured by the experimental uncertainty.

Finally, it might be argued that, since pressure breaks up ion pairs by increasing the dielectric constant of the medium, the $6\text{--}7 \text{ cm}^3 \text{ mol}^{-1}$ excess of the observed ΔV_{el}^\ddagger for $\text{AlW}_{12}\text{O}_{40}^{5-/6-}$ over the theoretical estimate might be accounted for through a reactive-ion-pair mechanism. Fuoss-type calculations,³⁴ however, predict a decline of only about 10% in K_{IP} from 0 to 200 MPa at typical experimental ionic strengths, which would give a positive contribution to ΔV_{el}^\ddagger of $1\text{--}2 \text{ cm}^3 \text{ mol}^{-1}$ at most.

The $\text{AlW}_{12}\text{O}_{40}^{5-/6-}$ Self-Exchange Reaction in Homogeneous Solution. The separate aqueous diamagnetic $\text{AlW}_{12}\text{O}_{40}^{5-}$ and paramagnetic $\text{AlW}_{12}\text{O}_{40}^{6-}$ ions showed sharp ^{27}Al resonances at $\delta_d = 72.9$ and $\delta_p = 74.7$ ppm, with half-widths at half-maximum $\Delta\nu_m^{d0} = 0.89 \pm 0.04$ and $\Delta\nu_m^{p0} = 0.88 \pm 0.07$ Hz, respectively, in good agreement with Geletii et al.¹⁴ The fact that these diamagnetic and paramagnetic ions have the same very narrow ^{27}Al line widths indicates that they are substitution-inert and that the odd electron in the reduced species occupies a molecular orbital covering the peripheral tungstate units but with zero electron density at the Al nucleus, which is in a site of high (T_d) symmetry.

Mixtures of $\text{AlW}_{12}\text{O}_{40}^{5-}$ with $\text{AlW}_{12}\text{O}_{40}^{6-}$ in aqueous NaCl ($[\text{Na}]_{\text{total}} = 0.125\text{--}1.025 \text{ mol L}^{-1}$) showed separate but exchange-broadened ^{27}Al resonances of line widths $\Delta\nu_m^d$ and $\Delta\nu_m^p$, respectively, with the broadening increasing with increasing $[\text{Na}^+]$ (cf. Geletii et al.¹⁴). In LiCl media, the broadening was less but still significant. Thus, chemical exchange in these systems was in the slow exchange limit on the ^{27}Al NMR time scale, and values k_{ex}^d and k_{ex}^p of the

(47) Marcus, Y. *Ion Properties*; Marcel Dekker: New York, 1997; Chapter 8.

(48) (a) Metelski, P. D.; Swaddle, T. W. *Inorg. Chem.* **1999**, *38*, 301. (b) Fu, Y.; Swaddle, T. W. *Inorg. Chem.* **1999**, *38*, 876.

Table 3. Effect of Supporting Electrolyte and Temperature on the Rate Constant k_{ex} for Self-Exchange of $\text{AlW}_{12}\text{O}_{40}^{5-}$ in Aqueous Solution^a

M salt ^b	[M salt]/ mol L ⁻¹	[M ⁺]/mol L ⁻¹	<i>I</i> /mol L ⁻¹	$k_{\text{ex}}/10^3 \text{ L mol}^{-1} \text{ s}^{-1}$ ^c	$\Delta H_{\text{ex}}^{\ddagger}/\text{kJ mol}^{-1}$	$\Delta S_{\text{ex}}^{\ddagger}/\text{J K}^{-1} \text{ mol}^{-1}$
LiCl	0.100	0.125	0.19	0.26 ± 0.01	9.1 ± 0.4	-168 ± 1
	0.200	0.225	0.29	0.53 ± 0.07	11.0 ± 0.7	-156 ± 2
	0.500 ^d	0.525	0.59	1.99 ± 0.08	16 ± 1	-127 ± 4
	1.000 ^d	1.025	1.09	5.67 ± 0.06	12.5 ± 0.8	-131 ± 3
NaCl	0.100	0.125	0.21	0.55 ± 0.01	4.0 ± 0.1	-179 ± 0.4
	0.200	0.225	0.32	1.7 ± 0.1	8.3 ± 0.5	-155 ± 2
	0.500	0.525	0.61	5.6 ± 0.1	4.5 ± 0.3	-160 ± 1
	1.000	1.025	1.12	12.9 ± 0.1	5.4 ± 0.3	-148 ± 1
KCl	0.100	0.125	0.22	9.8 ± 0.1	-3.8 ± 0.1	-181 ± 0.5
	0.200	0.225	0.32	24.0 ± 0.2	-5.3 ± 0.2	-179 ± 1
	0.500	0.525	0.61	62 ± 3	-7.4 ± 0.4	-178 ± 1
			0.62	61.6 ± 0.8	-6.4 ± 0.4	-175 ± 1
			1.09 ^e	128.6 ^e	-2.9 ± 0.1	-157 ± 0.2
KCF ₃ SO ₃	0.500 ^d	0.525	0.59	54 ± 5	-7.3 ± 1.0	-179 ± 3
	RbCl ^f	0.100	0.19	51.8 ± 0.1	-12.6 ± 0.8	-197 ± 3
Rb ₂ CO ₃ ^f	0.200 ^d	0.200	0.29	124 ± 5	-5.6 ± 0.3	-166 ± 2
	0.300 ^d	0.300	0.39	179 ^e		
	0.100 ^d	0.200	0.39	122 ± 5	-5.7 ± 0.5	-167 ± 2

^a Temperature 25.0 °C (k_{ex} for 10, 20, 30, and 40 °C are given in Table S7 in the Supporting Information); total $[\text{AlW}_{12}\text{O}_{40}^{5-}] = 5.0 \text{ mmol L}^{-1}$ except as noted. ^b $\text{M}_2\text{HPO}_4(25 \text{ mmol L}^{-1})/\text{MH}_2\text{PO}_4(25 \text{ mmol L}^{-1})$ buffer present except as indicated. ^c Average of values from deconvoluted $\text{AlW}_{12}\text{O}_{40}^{5-}$ and $\text{AlW}_{12}\text{O}_{40}^{6-}$ resonances in slow exchange regime, except as noted. ^d 1.0 mmol HCl present in place of phosphate buffer. ^e Resonances at or near coalescence; single rate constant from intermediate-exchange-rate equation, uncertainty $\sim \pm 5\%$. ^f Solution prepared from $\text{Li}_5\text{AlW}_{12}\text{O}_{40}$ (5 mmol L⁻¹); contribution of Li^+ -dependent pathway to k_{ex} is negligible.

electron-transfer rate constant k_{ex} can be calculated from the respective peak widths:⁴⁹

$$k_{\text{ex}}^{\text{d}} = \pi(\Delta\nu_{\text{m}}^{\text{d}} - \Delta\nu_{\text{m}}^{\text{d}0})/[\text{AlW}_{12}\text{O}_{40}^{5-}];$$

$$k_{\text{ex}}^{\text{p}} = \pi(\Delta\nu_{\text{m}}^{\text{p}} - \Delta\nu_{\text{m}}^{\text{p}0})/[\text{AlW}_{12}\text{O}_{40}^{6-}] \quad (12)$$

It was established (e.g., from the data of Table S8 for Na^+ as the cation) that k_{ex}^{d} and k_{ex}^{p} were effectively equal for $[\text{AlW}_{12}\text{O}_{40}^{5-}]:[\text{AlW}_{12}\text{O}_{40}^{6-}]$ ratios ranging from about 3:1 to 1:3 at a total reactant concentration 5.0 mmol L⁻¹). Thus, the exchange reaction was first-order with respect to both $\text{AlW}_{12}\text{O}_{40}^{5-}$ with $\text{AlW}_{12}\text{O}_{40}^{6-}$. The k_{ex} values listed in Table 3 are averages of k_{ex}^{d} and k_{ex}^{p} obtained for solutions in which $[\text{AlW}_{12}\text{O}_{40}^{5-}]:[\text{AlW}_{12}\text{O}_{40}^{6-}]$ was close to the optimum 1:1. In KCl media, the much faster exchange led to overlap and ultimately coalescence of the ²⁷Al resonances as $[\text{K}^+]$ was increased (Figure 3), and exchange in RbCl solutions was faster again. For $[\text{KCl}] = 0.5 \text{ mol L}^{-1}$ and $[\text{RbCl}] = 0.2 \text{ mol L}^{-1}$ at 25 °C, the k_{ex} values given in Table 3 were calculated from simulations of the line shape using the gNMR program (IvorySoft, v. 5.0.2.0). The gNMR program, however, assumes Lorentzian line shapes, which is not strictly correct for chemically exchanging systems. As a check, therefore, these spectra were deconvoluted using the Bruker XWINNMR program (v. 95.8.1.1), and k_{ex} was calculated from eq 12; this procedure is also flawed because the exchange rate obviously lies outside the slow exchange regime for which eq 12 is valid, but the two procedures gave k_{ex} values that agreed within $\sim 10\%$. For coalesced peaks of width W_{dp} , relating to equally populated exchanging sites, k_{ex} can be calculated from eq 13,⁴⁹ in which $\Delta\nu = \delta_{\text{p}} - \delta_{\text{d}}$ (in Hz):

$$k_{\text{ex}} = (\pi\Delta\nu/2)[(\Delta\nu/W_{\text{dp}})^2 - (W_{\text{dp}}/\Delta\nu)^2 + 2]^{1/2} \quad (13)$$

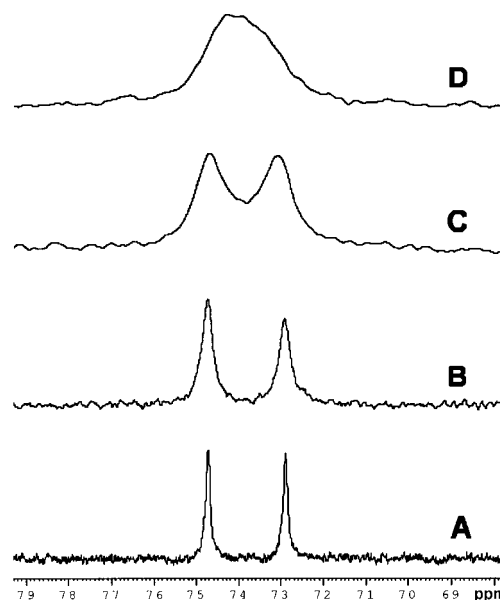


Figure 3. Exchange broadened ²⁷Al spectra of approximately equimolar mixtures of $\text{AlW}_{12}\text{O}_{40}^{6-}$ (left peak) and $\text{AlW}_{12}\text{O}_{40}^{5-}$ (right peak) in aqueous (20% D_2O) KCl media at 25.0 °C. $[\text{K}^+]_{\text{total}}/\text{mol L}^{-1} = 0.125$ (A), 0.225 (B), 0.525 (C), and 1.025 (D). $[\text{AlW}_{12}\text{O}_{40}^{5-}]_{\text{total}} = 5.0 \text{ mmol L}^{-1}$.

The rate constants k_{ex} for the $\text{AlW}_{12}\text{O}_{40}^{5-}/6-$ self-exchange reaction in NaCl media at 25.0 °C are in good agreement with those obtained by Geletii et al. at 19.2 °C over essentially the same range of $[\text{NaCl}]$,¹⁴ allowing for the small temperature dependence. Geletii et al.¹⁴ obtained a good fit of k_{ex} for NaCl media to a linearized form of eq 8 by fixing a at twice the radius of the $\text{AlW}_{12}\text{O}_{40}^{5-}$ anion (1.12 nm), rather than the sum of the hydrated radii of this anion and Na^+ as required by the extended Debye–Hückel and BBC theories. If a is treated as a free parameter, a nonlinear least-squares fit of the k_{ex} data of Geletii et al.¹⁴ to eq 8 gives a

(49) Sandström, J. *Dynamic NMR Spectroscopy*; Academic Press: London, 1982.

$= 1.14 \pm 0.03$ nm and the rate constant at hypothetical infinite dilution $k_{\text{ex}}^{I=0}$ at 19.2 °C $= 0.0034 \pm 0.0012$ L mol $^{-1}$ s $^{-1}$ (Figure S7 in the Supporting Information); Geletii et al.¹⁴ derived a substantially higher value, $k_{\text{ex}}^{I=0} = 0.0065 \pm 0.0015$ L mol $^{-1}$ s $^{-1}$, from the same data set with a fixed at 1.12 nm. When the k_{ex} data of Table 3 are fitted to eq 8 with variable a (Figure S8), the respective values of a/nm for LiCl, NaCl, and KCl media are 1.20 ± 0.03 , 1.16 ± 0.06 , and 1.30 ± 0.04 (that is, quite consistent and close to twice the $\text{AlW}_{12}\text{O}_{40}^{5-}$ radius), but the rate constant at infinite dilution varies unacceptably: $k_{\text{ex}}^{I=0}/\text{L mol}^{-1} \text{ s}^{-1} = 0.0029 \pm 0.0008$, 0.0048 ± 0.0029 , and 0.18 ± 0.06 , respectively, at 25.0 °C. In other words, the assumption made by Geletii et al.,¹⁴ that a may be set to twice the $\text{AlW}_{12}\text{O}_{40}^{5-}$ radius, happens to reproduce the curvature of plots of $\ln k_{\text{ex}}$ versus I according to eq 8 well enough but fails to account for the absolute values of k_{ex} , and in particular for the substantially elevated values seen for KCl (and KCF_3SO_3) media (for RbCl media, solubility limitations and high exchange rates prevented study of the self-exchange reaction over a sufficiently wide range of I).

Geletii et al.¹⁴ were encouraged by the good agreement found between the rate constant measured spectrophotometrically for the net reaction of $\text{AlW}_{12}\text{O}_{40}^{6-}$ with $\text{PW}_{12}\text{O}_{40}^{4-}$ and that obtained by applying their $k_{\text{ex}}^{I=0}$ value in the Marcus cross-relation. We caution, however, that (i) the long extrapolation necessary to obtain $k_{\text{ex}}^{I=0}$ (Figure S7) gives widely differing values depending on how the fitting to eq 8 or some alternative (e.g., quadratic) equation is done; (ii) the cation-specificity of k_{ex} evident in Table 3 leads to inconsistent $k_{\text{ex}}^{I=0}$ values on the basis of eq 8, whereas the same $k_{\text{ex}}^{I=0}$ value should be obtained at infinite dilution for all aqueous media if eq 8 is valid for these systems; and (iii) the phenomenon of cation-specificity of k_{ex} raises doubts about the applicability in these systems of the Marcus cross-relation, which assumes electron transfer between two spherical molecules or ions without intervention of a third species.

We conclude that eq 8 is inadequate to explain the medium dependence of k_{ex} , which clearly depends on the nature and concentration of M^+ rather than ionic strength as such. This was evident in an experiment using $1/2\text{Rb}_2\text{CO}_3$ rather than RbCl (Table 3), in which k_{ex} was the same despite the substantial difference in I ; this experiment also showed that k_{ex} was independent of pH even in the mildly alkaline regime. Equation 8 does at least indicate that $k_{\text{ex}}^{I=0}$ would be negligibly small relative to the k_{ex} values of Table 3 (cf. $k_{\text{el}}^{I=0}$). (An attempt was made to observe the uncatalyzed $\text{AlW}_{12}\text{O}_{40}^{5-}/6-$ self-exchange pathway by sequestering all the cation K^+ in a $\text{K}^+/\text{AlW}_{12}\text{O}_{40}^{5-}/6-/ \text{KCl}$ solution with crypt-2.2.2,⁵⁰ but a tungstoaluminate salt of $\text{K}(\text{crypt-2.2.2})^+$ precipitated.) Accordingly, as with the electrode reaction, the dependence of k_{ex} on $[\text{M}^+]$ is most usefully represented by a purely empirical power equation (eq 14, cf. eq 10; Figure 4), which allows one to summarize the data without extraneous assumptions and to assess the possible approach

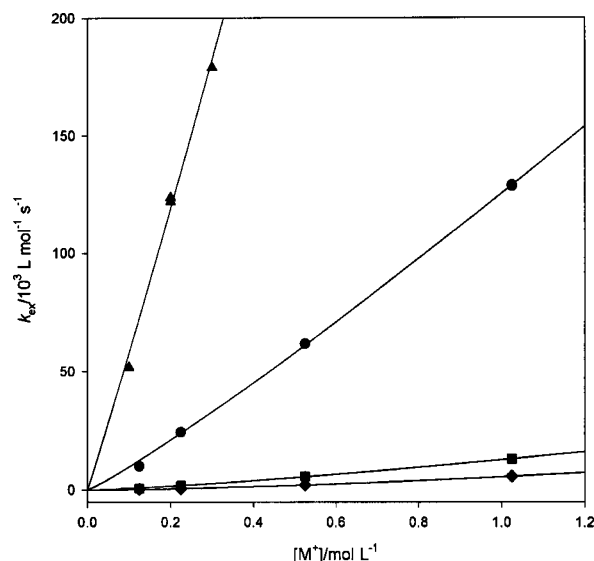


Figure 4. Dependence of k_{ex} for the $\text{AlW}_{12}\text{O}_{40}^{5-}/6-$ self-exchange reaction at 25.0 °C on the nature and concentration of the cation M^+ . $\text{M} = \text{Li}$ (\blacklozenge), Na (\blacksquare), K (\bullet), Rb (\blacktriangle). For $\text{M} = \text{Rb}$, the negligibly small contributions of the Li^+ counterion (0.025 mol L^{-1}) to k_{ex} have been subtracted.

to direct proportionality (exponent $p' = 1.0$) between k_{ex} and $[\text{M}^+]$, such as has been reported^{48a,50} for self-exchange reactions of some cyanometalate couples:

$$k_{\text{ex}} = m'[\text{M}^+]^{p'} \quad (14)$$

The strong catalytic effect of K^+ and Rb^+ is clearly evident in Figure 4. Nonlinear least-squares fits of k_{ex} to eq 14 gave $m'/\text{L}^{p'+1} \text{ mol}^{-p'-1} \text{ s}^{-1} = (5.45 \pm 0.03) \times 10^3$, $(1.25 \pm 0.02) \times 10^4$, $(1.26 \pm 0.09) \times 10^5$, and $(6.44 \pm 0.8) \times 10^5$, with $p' = 1.56 \pm 0.02$, 1.30 ± 0.05 , 1.12 ± 0.02 , and 1.05 ± 0.08 , for $\text{M} = \text{Li}$, Na , K , and Rb , respectively. The p' values show that k_{ex} approaches simple proportionality to $[\text{M}^+]$ (i.e., approximate first-order dependence on $[\text{M}^+]$) more closely as we go from Li to Rb, probably because the reaction rate is increasingly governed by specific cation catalysis to the exclusion of medium effects of the Debye–Hückel type as we go to cations that are more easily dehydrated (and, arguably, more polarizable).

Thus, for the K^+ and Rb^+ cases at least, the exchange reaction rate is essentially first order in the concentration of the cation as well as of each of the reacting anions, much as has been found for self-exchange reactions of several cyanometalates.^{1,48a,50} Exact conformity to first-order dependence on $[\text{M}^+]$ is not expected, particularly for the slower exchange reactions, as some vestiges of medium effects may be anticipated. Undoubtedly, some preassociation of the cation with one of the anions will precede a reactive encounter with the other, but this does not imply that equilibrium ion-pairing as conventionally conceived is the sole factor governing electrolyte effects on the exchange reaction rate. A relevant observation is that, within the experimental uncertainty, Figure 4 shows no evidence of saturation of the cation effect over the entire concentration range 0 – 1.025 mol L^{-1} . The Fuoss ion pair formation constants of Table S2 predict that pairing of the tungstoaluminate ions with M^+ should be substantial but incomplete.

(50) Zahl, A.; van Eldik, R.; Swaddle, T. W. *Inorg. Chem.* **2002**, *41*, 757.

For example, the fractions of $\text{AlW}_{12}\text{O}_{40}^{5-}$ and $\text{AlW}_{12}\text{O}_{40}^{6-}$ present as ion pairs with K^+ are predicted to range from 58% to 81% and from 69% to 84%, respectively, of the totals ($\sim 2.5 \text{ mmol L}^{-1}$ each in all cases) over the whole $[\text{K}^+]$ range ($0.125\text{--}1.025 \text{ mol L}^{-1}$); thus, the ion pair concentrations vary much more slowly than the total $[\text{K}^+]$ itself (because K_{IP} falls as I increases) and are tending to saturation. Consequently, insofar as the Fuoss model is realistic, if the kinetic effect of M^+ were due solely to ion pairing in some way, the exponent p' would be much less than 1.0 and curvature of Figure 4 toward a saturation value of k_{ex} would be evident. More significantly, there should, according to Table S2, be much less difference between k_{ex} for Na^+ , K^+ , and Rb^+ than is observed. Thus, while ion pairing may well be extensive, the accelerating effect of M^+ on the $\text{AlW}_{12}\text{O}_{40}^{5-/6-}$ self-exchange reaction cannot be attributed to it alone.

A cursory glance at Figure 4 might suggest that a change in mechanism occurs on going from Li^+ and Na^+ to K^+ and Rb^+ . This, however, is an illusion due to the linear scaling of k_{ex} . The key point is that, in all four cases, k_{ex} is roughly first-order in $[\text{M}^+]$ with a zero intercept but with marked differences in the degree of the catalytic effect of M^+ . In the latter respect, Li^+ and Na^+ are significantly different from each other as well as from K^+ and Rb^+ .

An unusual feature of the M^+ -mediated $\text{AlW}_{12}\text{O}_{40}^{5-/6-}$ self-exchange is that $\Delta H_{\text{ex}}^\ddagger$ goes from small positive values for LiCl and NaCl media to small negative values for KCl and RbCl solutions (Table 3). The direction of the trend, $\text{M} = \text{Li} > \text{Na} > \text{K} > \text{Rb}$, and of a partially compensating trend in the strongly negative $\Delta S_{\text{ex}}^\ddagger$, reflects that for the corresponding electrode reaction (Figure 2), and its smoothness is consistent with a single common self-exchange mechanism for all these cations as catalysts. The essential point is that the free energy of activation $\Delta G_{\text{ex}}^\ddagger (= \Delta H_{\text{ex}}^\ddagger - T\Delta S_{\text{ex}}^\ddagger)$, which determines $\ln k_{\text{ex}}$, remains positive even for negative $\Delta H_{\text{ex}}^\ddagger$ because of the strongly negative $\Delta S_{\text{ex}}^\ddagger$. The latter reflects the high degree of organization required to reach the $\text{AlW}_{12}\text{O}_{40}^{5-} - \text{M}^+ - \text{AlW}_{12}\text{O}_{40}^{6-}$ transition state.

Near-zero and negative values of ΔH^\ddagger are not unprecedented in fast electron-transfer reactions between metal complexes.^{51–57} They may arise if the combined enthalpy changes for all steps in the formation of a precursor complex from the reactants are at least as negative as the enthalpy of activation for conversion of the precursor to the successor complex is positive⁵⁶ (other explanations have been advanced^{53,54}). Ion pairing to form $\{\text{M}^+, \text{AlW}_{12}\text{O}_{40}^{6-}\}$ and to a lesser extent $\{\text{M}^+, \text{AlW}_{12}\text{O}_{40}^{5-}\}$ may assist in this. Intercession of M^+ lowers the enthalpy of the $\text{AlW}_{12}\text{O}_{40}^{5-/6-}$ pair when the precursor complex is formed, and also reduces greatly the enthalpy of activation for electron transfer within

that complex. The effectiveness of M^+ , especially in the latter step, is expected to be increased if it becomes partially dehydrated somewhere along the reaction coordinate to permit closer approach of the reactant anions,⁴⁸ leading to the observed sequence of catalytic effectiveness $\text{Li}^+ < \text{Na}^+ < \text{K}^+ < \text{Rb}^+$, which is the order in which the heats of hydration of M^+ become less negative. This is also the order of increasing polarizability of M^+ , which might be considered to facilitate electron transfer via M^+ . The latter possibility could be dismissed if the poorly polarizable tetraalkylammonium ions could be shown to be about as effective as K^+ or Rb^+ in catalyzing the $\text{AlW}_{12}\text{O}_{40}^{5-/6-}$ exchange,⁵⁸ as is the case for cyanometalate self-exchange reactions,^{48,50} but when attempting this we found that tetramethyl-, tetraethyl-, and tetra-*n*-butylammonium $\text{AlW}_{12}\text{O}_{40}^{5-}$ salts are too poorly soluble.⁵⁹

Measurements of $\Delta V_{\text{ex}}^\ddagger$ for the M^+ -catalyzed homogeneous $\text{AlW}_{12}\text{O}_{40}^{5-/6-}$ self-exchange reaction were planned to test the M^+ dehydration model⁴⁸ but were abandoned because of the high sensitivity of $\text{AlW}_{12}\text{O}_{40}^{6-}$ to traces of O_2 , which is difficult to exclude rigorously when setting up high-pressure NMR experiments. Ironically, the effects of O_2 were most marked in the presence of the same cations (K^+ and Rb^+) that are of most interest as catalysts for the self-exchange reaction, presumably because cross reactions of the $\text{AlW}_{12}\text{O}_{40}^{5-/6-}$ couple with redox reagents are susceptible to cation catalysis in the same way as is self-exchange (cf. redox reactions of cyanometalate anions, e.g., the M^+ -catalyzed oxidation of anionic, cationic, and neutral forms of ascorbic acid⁶⁰).

Conclusions. For the aqueous $\text{AlW}_{12}\text{O}_{40}^{5-/6-}$ couple at a gold electrode at pH 3 and 25 °C, the curvature of plots of the liquid-junction-corrected midpoint potentials E_{corr} against ionic strength I can be satisfactorily represented by an adaptation of the extended Debye–Hückel equation (eq 2 and Figure 1) if the ion size parameter a is treated as an adjustable parameter, although a small dependence of the apparent infinite-dilution potential E_{corr}^0 , and hence of the absolute values of E_{corr} , on the nature of the alkali metal cation M^+ persists. If a is fixed as the sum of the radius of $\text{AlW}_{12}\text{O}_{40}^{5-}$ and the hydrodynamic radius of M^+ , as theory requires, eq 2 fails unless an empirical term cI is added, which gives improved agreement in E_{corr}^0 , but the interpretational problem then becomes one of explaining the variation of c with the identity of M^+ . According to the Fuoss treatment, ion pairing does not account for the inadequacies of eq 2. In any event, the importance of ion pairing in water, even for these highly charged tungstoaluminate anions, is likely to be less than intuitively expected because the effect of high electrolyte concentrations that favor ion pairing will

(51) Sutin, N.; Gordon, B. M. *J. Am. Chem. Soc.* **1961**, *83*, 70.
 (52) Braddock, J. N.; Meyer, T. J. *J. Am. Chem. Soc.* **1973**, *95*, 3158.
 (53) Cramer, J. L.; Meyer, T. J. *Inorg. Chem.* **1974**, *13*, 1250.
 (54) Marcus, R. A.; Sutin, N. *Inorg. Chem.* **1975**, *14*, 213.
 (55) Frank, R.; Greiner, G.; Rau, H. *Phys. Chem. Chem. Phys.* **1999**, *1*, 3481.
 (56) Fukuzumi, S.; Endo, Y.; Imahori, H. *J. Am. Chem. Soc.* **2002**, *124*, 10974.
 (57) Yoder, J. C.; Roth, J. P.; Gussenhoven, E. M.; Larsen, A. S.; Mayer, J. M. *J. Am. Chem. Soc.* **2003**, *125*, 2629.

(58) Cannon, R. D. *Electron-Transfer Reactions*; Butterworth: London, 1980; p 226.
 (59) For example, the point of formation of a permanent precipitate during dropwise addition of Et_4NBr solution (0.025 mol L^{-1}) to $\text{Na}_5[\text{AlW}_{12}\text{O}_{40}]$ solution (0.01 mol L^{-1}) placed an upper limit of $1 \times 10^{-15} \text{ mol}^6 \text{ L}^{-6}$ on the solubility product of $(\text{Et}_4\text{N})_5[\text{AlW}_{12}\text{O}_{40}]$ at 23 °C, corresponding to a solubility of $\leq 0.0008 \text{ mol L}^{-1}$ for the latter salt alone in water.
 (60) Leal, J. M.; Domingo, P. L.; García, B.; Ibeas, S. *J. Chem. Soc., Faraday Trans.* **1993**, *89*, 3571.

be offset by a diminution of the ion pair formation constants through increasing ionic strength. It may be concluded that the extended Debye–Hückel approach is not quantitatively valid in the electrolyte concentration ranges of our experiments or those of Kozik and Baker¹⁰ and Geletii et al.,¹⁴ and that ion pairing alone is insufficient to account for the deviations.

The volumes of reaction $\Delta V_{\text{Ag/AgCl}}$ for the $\text{AlW}_{12}\text{O}_{40}^{5-/6-}/\text{Ag/AgCl}$ cell are of a magnitude relative to those of other couples that is at least qualitatively consistent with the expectations of the Born–Drude–Nernst theory.

The dependence of the $\text{AlW}_{12}\text{O}_{40}^{5-/6-}$ electrode reaction rate constants k_{el} on the identity of M^+ is pronounced, even at 0.1 mol L^{-1} , but an adaptation of the Debye–Hückel-based BBC equation (eq 8) for electrode processes (eq 9) again requires unrealistic values of the ionic close-approach distance a to match the curvature of $\ln k_{\text{el}}$ plots, and furthermore gives inconsistent values of $k_{\text{el}}^{I=0}$ for the various M^+ . For the homogeneous self-exchange reaction, the BBC equation reproduces the curvature of $\ln k_{\text{ex}}$ versus I plots, but nonlinear least-squares fitting again gives inconsistent values of $k_{\text{ex}}^{I=0}$ for the different M^+ and unrealistic values of a ; in this case, a is roughly the same for all M^+ and fortuitously similar to twice the radius of $\text{AlW}_{12}\text{O}_{40}^{5-}$ rather than the sum of the cation–anion radii; i.e., it fails to account for the specific effects of M^+ on k_{ex} evident in Figure 4.

Monk,⁶¹ in commenting on a controversy over the utility of Debye–Hückel theory and the ionic strength concept, remarked that there is a need for improved theoretical treatments of electrolyte effects on reaction rates of transition metal complexes (inter alia), and this is clearly true. Invocation of ion-pairing to extend Debye–Hückel theory to ionic strengths above 0.1 mol L^{-1} is unlikely to succeed because ion-pair formation constants are themselves subject to Debye–Hückel-type effects. Nevertheless, over and above any medium effects of the Debye–Hückel sort, there remains in the kinetics of the $\text{AlW}_{12}\text{O}_{40}^{5-/6-}$ electron-transfer reactions a specific catalytic effect of M^+ that implies a reaction mechanism involving M^+ explicitly.

As for representation of the data, extrapolation of k_{ex} to infinite dilution using eq 8, as applied to Na^+ media by Kozik and Baker¹⁰ and Geletii et al.,¹⁴ gives substantially different results for different M^+ , which is unacceptable. Nevertheless, extrapolations using eq 8, or quadratic regressions of k_{el} or k_{ex} on $[\text{M}^+]$, indicate that $k_{\text{el}}^{I=0}$ and $k_{\text{ex}}^{I=0}$, which should represent the rate constants for the uncatalyzed reactions, are negligibly small relative to the respective k_{el} and k_{ex}

values of Tables 1 and 3. Accordingly, simple near-linear power dependences of both k_{el} and k_{ex} on $[\text{M}^+]$ (eqs 10 and 14) serve to represent the data empirically, to indicate that the exchange reaction is roughly first-order in $[\text{M}^+]$ as well as in $[\text{AlW}_{12}\text{O}_{40}^{5-}]$ and $[\text{AlW}_{12}\text{O}_{40}^{6-}]$, consistent with specific M^+ catalysis, and to emphasize that the effect of M^+ shows no sign of saturation up to $[\text{M}^+] \sim 1.1 \text{ mol L}^{-1}$ at least, which indicates that the effect is not simply one of ion pairing.

For both k_{el} and k_{ex} , the activation parameters governing the temperature and (for k_{el}) pressure dependences of the reaction rate are consistent with a mechanism previously proposed^{1,2,48} according to which electron transfer between anions, either in homogeneous aqueous solution or at an electrode, is catalyzed by M^+ in a partially dehydrated state, thus explaining the observed sequence of catalytic efficacy $\text{M} = \text{Li} < \text{Na} < \text{K} < \text{Rb}$. In the absence of $\Delta V_{\text{ex}}^\ddagger$ data because of technical difficulties, this interpretation remains more speculative than we would wish. Nevertheless, the approximate first-order dependence of the exchange rates on the stoichiometric $[\text{M}^+]$ is consistent with the requirement of the presence of a small fraction of M^+ in partially dehydrated form for the reaction to proceed readily; this fraction would be largely independent of Debye–Hückel or ion-pairing effects. For both the electrode and the homogeneous self-exchange reactions, catalysis by M^+ leads to enthalpies of activation that are small and diminish in the sequence $\text{M} = \text{Li} > \text{Na} > \text{K} > \text{Rb}$, such that $\Delta H_{\text{ex}}^\ddagger$ in particular actually becomes negative for $\text{M} = \text{K}$ and Rb . The low activation enthalpies are partially compensated by strongly negative entropies of activation; thus, the catalytic effect of M^+ is enthalpic in origin and limited entropically.

Acknowledgment. We thank Drs. Yu. Geletii, C. L. Hill, and I. A. Weinstock for much helpful advice, and the Natural Sciences and Engineering Research Council Canada for financial support.

Supporting Information Available: Sketch of electrochemical cell; sample plots of $\ln k_{\text{el}}$ vs pressure; plots of E_{corr} , k_{el} and k_{ex} against electrolyte concentration according to eqs 4 and 8–10; tables relating to liquid-junction potentials, calculated temperature dependence of diffusion coefficients, theoretical ion-pair formation constants, electrochemical transfer coefficients, uncompensated resistance, rate constants k_{ex} as a function of temperature, and thermal activation parameters for the electrode reaction. This material is available free of charge via the Internet at <http://pubs.acs.org>.

(61) Monk, C. B. *Chem. Br.* **1993**, 29, 1033 and references therein.